



HAL
open science

Non-Linear control for car like mobile robots in presence of sliding: application to guidance of farm vehicles using a single RTK GPS

Roland Lenain, Benoit Thuilot, Christophe Cariou, Philippe Martinet

► To cite this version:

Roland Lenain, Benoit Thuilot, Christophe Cariou, Philippe Martinet. Non-Linear control for car like mobile robots in presence of sliding: application to guidance of farm vehicles using a single RTK GPS. 35th International Symposium on Robotics ISR, Paris, 23 March 2004, Mar 2004, Paris, France. pp.6. hal-02467053

HAL Id: hal-02467053

<https://inria.hal.science/hal-02467053>

Submitted on 4 Feb 2020

HAL is a multi-disciplinary open access archive for the deposit and dissemination of scientific research documents, whether they are published or not. The documents may come from teaching and research institutions in France or abroad, or from public or private research centers.

L'archive ouverte pluridisciplinaire **HAL**, est destinée au dépôt et à la diffusion de documents scientifiques de niveau recherche, publiés ou non, émanant des établissements d'enseignement et de recherche français ou étrangers, des laboratoires publics ou privés.

Non-Linear control for car like mobile robots in presence of sliding:

Application to guidance of farm vehicles using a single RTK GPS

Roland Lenain[◇], Benoit Thuilot^{*}, Christophe Cariou[◇], Philippe Martinet^{*}
[◇] Cemagref ^{*} LASMEA

BP50085 - 24, av. des Landais
63172 Aubière Cedex France
roland.lenain@cemagref.fr

24, av. des Landais
63177 Aubière Cedex France
benoit.thuilot@lasmea.univ-bpclermont.fr

Abstract—Since Global Navigation Satellite Systems are able to supply very accurate coordinates of a point (about 2 cm with a RTK GPS), such a sensor is very suitable to design vehicle guidance system. It is especially the case in agricultural tasks where a centimeter precision is often required (seeding, spraying, ...). To answer to growing high precision agriculture principle demand, several control laws for automated vehicle guidance relying on this sensor have been developed. Such guidance systems are able to supply an acceptable steering accuracy as long as vehicle does not slide (path tracking on even ground with good adherence properties...), what alas inevitably occurs in agricultural tasks. Several principles are here presented to steer vehicle whatever properties of ground and path to be followed are. In this paper two extended kinematic models with sliding accounted are presented. They allow to describe vehicle dynamics in all guidance conditions. Via these models, new non linear control laws can be designed (depending on model structures), which integrate sliding effects. Their capabilities are investigated through experimental tests.

I. INTRODUCTION

As precision agriculture principles have been taking more and more importance in industrialized world and since improvement of GNSS (Global Navigation Satellite Systems) allows more and more accurate positioning data with a reducing cost, researches on automated vehicle guidance are meeting user interest, in particular in agricultural area. Moreover such systems can reduce hardness of farmer's work and improve his yield rate. As our application domain concerns vehicles working on open fields, there is no obstacle (such as buildings, or trees, ...) to disturb satellites receiving and use of a unique RTK GPS to perform a guidance task appears to be very suitable (as it has been shown in [12]).

Several research teams have been developing such systems with different performances and for dedicated applications. For the moment, only few devices are manufactured (by John Deere or CLAAS for example, ...), which are dedicated to perform specific tasks (straight line following for John Deere or harvesting for CLAAS) and can not be used for general path following. Moreover, most of them use several exteroceptive sensors (four GPS antennas in [8], RTK GPS and inertial sensor in [7], fusion between GPS and vision in [9] and [11]) to improve tracking and let control scheme be independent from sliding even if models do not take it into account.

Our approach uses only one main sensor (Real Time Kinematic GPS) which necessitates to take sliding effects into account to

preserve an acceptable tracking accuracy (as it is shown in [5]). A first idea to integrate such phenomenon inside control scheme could be the development of a dynamic model of vehicle which could take into account condition of rolling with sliding on each wheel as it has been done in [3]. Unfortunately several dynamic parameters such as tire adherence coefficient are very hard to get with sufficient accuracy and must be, in agricultural fields, evaluated on line. This can not be done efficiently in our application, and control methods have to be based on a kinematic model.

In this paper, two extended kinematic models used to describe vehicle dynamics in presence of sliding are presented and validated. These models allow to build control laws including sliding which are able to improve path following accuracy. Full scale experiments are discussed and demonstrate capability of such control schemes to follow with accuracy a reference path, whatever its shape and whatever the ground on which vehicle evolves.

II. EXPERIMENTAL BACKGROUND

This paper deals with actual experiments carried in partnership with manufacturer CLAAS. Figure 1 shows experimental vehicles (an Ares 640 tractor from RENAULT-Agriculture and a Dominator combine harvester from CLAAS) on which are tested control laws developed to perform automatic guidance applications. In this paper, all experiments described have been performed on tractor and control law description is relevant for the tractor (in the combine harvester case, since the steering axle is the rear one, sign modifications have to be introduced, but the control principles can be preserved).

The main sensor used to ensure control is a RTK GPS man-



Fig. 1. Vehicle used for actual experiments

ufactured by Thales Navigation (Aquarius 5002 unit shown

on figure 2) which supplies a positioning signal, with a 2cm accuracy, at a 10Hz sampling frequency. Mobile antenna is placed on the top of the vehicle straight up the center of rear axle (since it is the vehicle control point as described in kinematic model). In addition to absolute coordinates informations, sensor system implemented on vehicle allows to access to several other data:

- Vehicle velocity: provided by GPS sensor.
- Vehicle heading: estimated via a Kalman filter which uses mobile robot evolution model fed by steering angle information and vehicle velocity.



Fig. 2. RTK GPS main sensor implemented on vehicle

III. KINEMATIC MODELLING

A. Notations and model without sliding

As our objective consists in path following, parameters of model are tracking oriented. Position and orientation of vehicle are so described compared to the path to be followed. Figure 3 shows this description. Vehicle is viewed as a bicycle (as in celebrated Ackermann model described for example in [13]). Parameters used to build model without sliding are hereafter listed:

- \mathcal{C} is the path to be followed,
- O is the center of vehicle virtual rear wheel,
- M is the point on \mathcal{C} which is the closest to O .
 M is assumed to be unique, which is realistic when the vehicle remains quite close from \mathcal{C} .
- s is the curvilinear coordinate of point M along \mathcal{C} , and $c(s)$ denotes the curvature of \mathcal{C} at that point.
- y and $\tilde{\theta}$ are respectively lateral and angular deviation of the vehicle with respect to reference path \mathcal{C} (see Figure 3).
- δ is the virtual front wheel steering angle.
- v is the vehicle linear velocity, considered here as a parameter, whose value may be time-varying during the vehicle evolution.
- L is the vehicle wheelbase.

Using these notations and under rolling without sliding condition of tires on the ground, evolution of vehicle with respect to the path to be followed can be described by model (1) as calculated in [10].

$$\begin{cases} \dot{s} &= \frac{V \cos(\tilde{\theta})}{1-c(s)y} \\ \dot{y} &= V \sin(\tilde{\theta}) \\ \dot{\tilde{\theta}} &= V \left[\frac{\tan(\delta)}{L} - \frac{c(s) \cos(\tilde{\theta})}{1-c(s)y} \right] \end{cases} \quad (1)$$

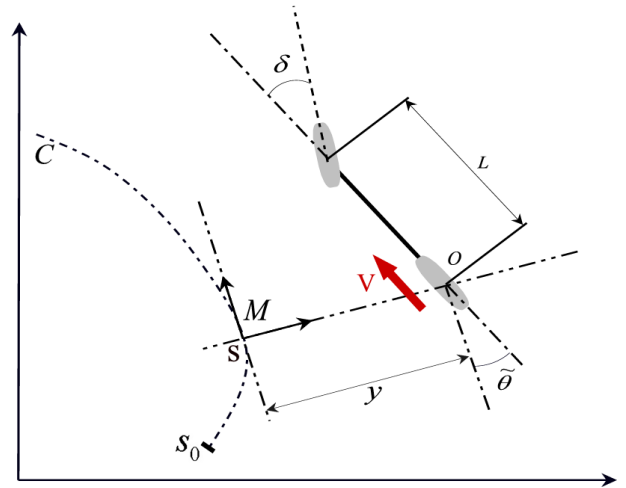


Fig. 3. Classical kinematic model parameters

B. First sliding model: Vehicle Behavior Description (VBD)

This approach, detailed in [5], takes into account sliding forces coming from dynamic studies and integrates them into kinematic model. As we do not control longitudinal movement, we consider only lateral dynamics. Sliding occurs when lateral forces applied by tires on ground are too important to be compensated by ground. In this case it is possible to consider a non compensated force on each tire (sliding resultant). As we consider vehicle as a bicycle, only two non compensated sliding resultant are taken into account: one applied on front axle and one on rear one (as described on figure 4).

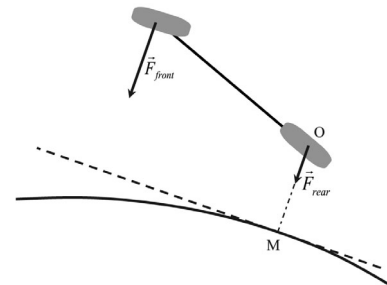


Fig. 4. Forces applied on vehicle wheels

This two forces (\vec{F}_{front} and \vec{F}_{rear}) have same direction but different values which implies two sliding movements: translation in the same direction as y , and a rotation movement around the same axis as $\tilde{\theta}$. Sliding can so be integrated inside kinematic model by adding two parameters to model without sliding (1): \dot{Y}_p for translation and $\dot{\Theta}_p$ for rotation, which denote the two sliding movements. Sliding model based on vehicle behavior description (VBD) is described by system (2).

$$\begin{cases} \dot{s} &= \frac{v \cos \tilde{\theta}}{1-c(s)y} \\ \dot{y} &= v \sin \tilde{\theta} + \dot{Y}_p \\ \dot{\tilde{\theta}} &= v \left(\frac{\tan \delta}{L} - \frac{c(s) \cos \tilde{\theta}}{1-c(s)y} \right) + \dot{\Theta}_p \end{cases} \quad (2)$$

C. Second sliding model: Tire Behavior Description (TBD)

Figure 5 shows a second set of parameters we can choose to describe sliding influence into kinematic model. This sliding description meets theory of vehicle dynamics partially described in [1], [2], and behavior of a tire as described in [3].

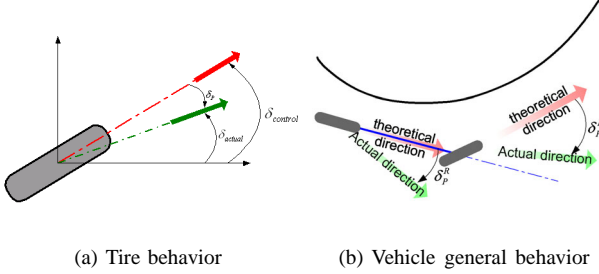


Fig. 5. Sliding parameters to be used in TBD kinematic model

Figure 5(a) shows that the actual speed vector orientation at tire center for a given steering angle is different from direction given by this steering angle. Elasticity of tire material (pseudo-sliding) and non verification of rolling without sliding condition (skidding) generate a cornering angle called here δ_P , which denotes difference between expected tire speed vector direction (given by steering angle) and actual one. This tire behavior modifies general vehicle dynamics as described on figure 5(b), where each of the two tires has an actual speed vector direction different from theoretical one. Instead of being a standard car like vehicle model, this description becomes closer to a two steering axes mobile robot, where front steering angle consists in an actual angle and a cornering one and rear steering angle reveals rear cornering angle.

Relying on this remark, it can then be shown that vehicle dynamics, described with respect to a local frame attached to the closest point of the reference path (see figure 3), can be described (see [6] for instance) by equations (3) which constitute sliding model based on tire behavior description (TBD).

$$\begin{cases} \dot{s} &= \frac{V \cos(\tilde{\theta} + \delta_P^R)}{1 - c(s)y} \\ \dot{y} &= V \sin(\tilde{\theta} + \delta_P^R) \\ \dot{\tilde{\theta}} &= V \left[\cos \delta_P^R \frac{\tan(\delta + \delta_P^R) - \tan \delta_P^R}{L} - \frac{c(s) \cos(\tilde{\theta} + \delta_P^R)}{1 - c(s)y} \right] \end{cases} \quad (3)$$

D. Sliding parameters estimation

One main problem in the two approaches chosen is estimation of sliding. The two sets of parameters here before introduced have to be estimated on line, as they are not constant, due to various and time varying parameters (steering angle, ground properties, slope, ...). Moreover, since we use a unique exteroceptive sensor, we must assume that all vehicle dynamics can be described using one of sliding model (VBD or TBD). Several dynamic behaviors are so ignored in models (such as roll or pitch) but their effects on path tracking

accuracy are considered negligible with respect to sliding and pseudo sliding.

Using this assumption, estimation is done by comparison between expected vehicle behavior using model under rolling without sliding condition (1) and actual vehicle dynamics, as described on scheme depicted on figure 6. An internal model of vehicle in rolling without sliding condition is so used to evaluate sliding parameters for both of models.

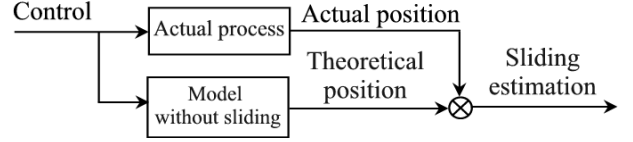


Fig. 6. Sliding detection

IV. VALIDATION OF MODELS

To validate relevance of models here before described, let us introduce the classical control used for vehicle in rolling without sliding condition. This allows us to compare actual behavior of vehicle and simulated one using both of sliding models when control does not take sliding into account.

A. Steering law design without sliding accounted

It has been established that most of mobile robots kinematic models can be converted, *without any approximation*, into almost linear models named chained forms, see for instance [10]. Such an approach is attractive, since control laws can then be designed according to Linear Systems Theory, while still relying upon the actual nonlinear mobile robots kinematic models.

More precisely, nonlinear kinematic model is first converted into chained form via invertible state and control nonlinear transformations. A linear control law is then designed relying on the chained form. Finally, the actual control law is computed via state and control nonlinear transformations. In [12], this technique is applied to kinematic model (1). It is shown that curved path following (i.e. maintaining y and $\tilde{\theta}$ equal to 0) can be achieved according to nonlinear control law:

$$\delta(y, \tilde{\theta}) = \arctan \left(L \left[\frac{\cos^3 \tilde{\theta}}{(1 - c(s)y)^2} \left(\frac{dc(s)}{ds} y \tan \tilde{\theta} - K_d (1 - c(s)y) \tan \tilde{\theta} - K_p y + c(s)(1 - c(s)y) \tan^2 \tilde{\theta} \right) + \frac{c(s) \cos \tilde{\theta}}{1 - c(s)y} \right] \right) \quad (4)$$

Where K_p and K_d can be interpreted as parameters of a PD controller. The new control law proposed in this paper will be exposed in section V.

B. Models validation relying on actual experiments

Here are now described results of sliding models simulation fed on-line during an actual path following, achieved with control law without sliding accounted (4). For both of sliding models, actual measurement data feed sliding estimation algorithm depicted on figure 6 to evaluate sliding parameters, which are injected in an on-line simulator to provide a simulated lateral deviation using both of sliding models. Figure (7) depicts path

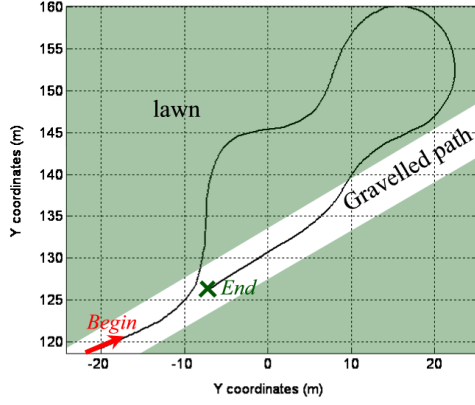


Fig. 7. Actual Path followed to validate models

stored on ground presenting low adherence properties. Results are presented on figure 8 where are depicted :

- in green dashed dot line, the vehicle actual lateral deviation during the path following,
- in blue solid line, simulation relying on VBD sliding model (2)
- in black dashed line, simulation relying on TBD sliding model (3)

We can see that the three lateral deviations depicted are very close. The two sliding models are so able to describe with accuracy vehicle dynamics, what is a first step to take it into account in control design. the slight differences between simulation of the two models are due to sliding estimation algorithms which do not compute sensor noise in the same way.

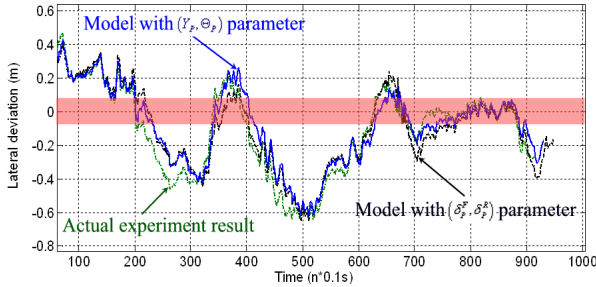


Fig. 8. Comparison between models and actual vehicle dynamics

C. Comparison of models

The TBD sliding model (3) denotes that sliding occurring during agricultural tasks is due to own vehicle movement and is linked to vehicle velocity. On the contrary, in VBD sliding model (2), sliding parameters are independent from vehicle configuration, so there is no mathematical restriction on sliding parameters in that model: it allows therefore the vehicle to be submitted to sliding effects which can not be compensated (i.e. $|\dot{Y}_p| > |v \sin \tilde{\theta}|$, phenomenon which is not addressed in our applications).

Under the relation here before introduced, it is possible to obtain mathematical relations (depending on vehicle configurations $\tilde{\theta}$ and δ) between the two sets of sliding parameters: this shows equivalence of models (3) and (2) (corroborated by simulation with theoretical sliding parameters).

The main difference between the two models is the integration level of sliding effects inside vehicle description: it acts on how sliding is viewed and can be corrected. While sliding effects in VBD model (2) are accounted by adding parameters on vehicle motion equations, they are integrated in nonlinear evolution equations in TBD model (3). From a control point of view, the advantage of this second model is that it is in a suitable form to be exactly linearized (chained system) with sliding accounted.

V. CONTROL DESIGN

A. Using VBD sliding model: adaptive control

VBD sliding model (2) is not under a suitable form to be turned into an almost linear system (called chained system, see control law here after defined or description of such form in [10]). To correct lateral deviation appearing when sliding occurs, we use adaptive control principle. As detailed in [5] When sliding is constant (\dot{Y}_p and $\dot{\Theta}_p$ constants) we notice that lateral deviation y resulting of control law (4) is constant too and can be calculated by equation (5). It is then possible to make vehicle converge to a null lateral deviation ($y = 0$) by applying an offset (called hereafter y_c) on input of control law (applying $\delta(y + y_c, \tilde{\theta})$ instead of $\delta(y, \tilde{\theta})$). Scheme depicted on figure 9 details such an adaptive control described.

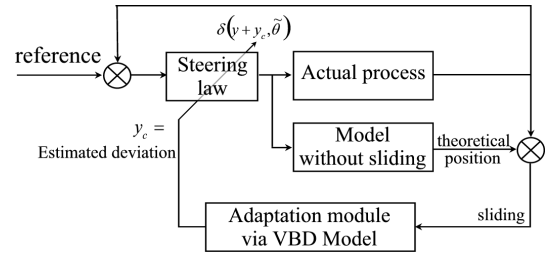


Fig. 9. Scheme of adaptive control method using VBD model

In cases studied, sliding is not constant but is evaluated on line. Moreover, VBD model is able to supply an estimation of the lateral deviation which occurs under control law (4). Output of VBD model is then used as an evaluation of the correction parameter y_c . More precisely, there is two ways to evaluate y_c : simulating on line the vehicle with VBD model or using the results of convergence calculation equation (5).

$$y \xrightarrow{t \rightarrow \infty} - \frac{\beta(s) + \frac{\dot{\Theta}_p}{v \cos^3 \tilde{\theta}}}{\alpha(s) - \frac{2c(s)\dot{\Theta}_p}{v \cos^3 \tilde{\theta}}} \triangleq y_c \quad (5)$$

where:

$$\begin{aligned} \tilde{\theta} &= -\arcsin\left(\frac{\dot{Y}_p}{v}\right) \\ \alpha(s) &= \frac{dc(s)}{ds} \tan \tilde{\theta} + c(s) \tan \tilde{\theta} (K_d - c(s) \tan \tilde{\theta}) - K_p \\ \beta(s) &= \tan \tilde{\theta} (c(s) \tan \tilde{\theta} - K_d) \end{aligned}$$

B. Using TBD sliding model: chained system control

As it has been already pointed out, TBD sliding model has a classical structure of car like mobile robot with two steering axles and can then easily be turned into a chain system to design a control law including TBD set of sliding parameters. This control design is hereafter detailed.

1) *Chained system conversion*: As developed in [10], one way to build a nonlinear suitable control law for mobile robots is to turn their equations into chained form (as it has been done, in order to design control law (4)). In dimension 3 (as expected in our application), such a system is given by :

$$\begin{cases} \dot{a}_1 &= m_1 \\ \dot{a}_2 &= a_3 m_1 \\ \dot{a}_3 &= m_2 \end{cases} \quad (6)$$

where $A = [a_1, a_2, a_3]^T$ and $M = [m_1, m_2]^T$ are resp. the state and control vectors. One can check that such a system is almost linear: just replace time derivation by a derivation with respect to a_1 . It leads to system (7) (with notation $a'_i = \frac{da_i}{da_1}$).

$$\begin{cases} a'_1 &= 1 \\ a'_2 &= a_3 \\ a'_3 &= m_3 = \frac{m_2}{m_1} \end{cases} \quad (7)$$

By analogy with chained transformations proposed for car like vehicle in the rolling without sliding case, the following state transformation $(s, y, \theta) \rightarrow (s, y, \tan(\tilde{\theta} + \delta_P^R) [1 - c(s)y])$ is here proposed in association with control transformation given by (8):

$$\begin{cases} m_1 &= \frac{V \cos(\tilde{\theta} + \delta_P^R)}{1 - c(s)y} \\ m_2 &= \frac{d}{ds} \left(\tan(\tilde{\theta} + \delta_P^R) [1 - c(s)y] \right) \end{cases} \quad (8)$$

According to equation (8), calculation of control m_2 implies derivation of sliding parameter δ_P^R . However, δ_P^R is estimated via estimation algorithm (figure 6). For convenient reasons this time varying parameter will be threaten as a constant. Such an approximation appears to be relevant during experiments. Using this hypothesis, calculation of m_2 gives us, under existence conditions:

$$\begin{aligned} m_2 &= -c(s)V \sin(\tilde{\theta} + \delta_P^R) \tan(\tilde{\theta} + \delta_P^R) \\ &+ \frac{1 - c(s)y}{\cos^2(\tilde{\theta} + \delta_P^R)} V \left[\cos \delta_P^R \left(\frac{\tan(\tilde{\theta} + \delta_P^R) - \tan \delta_P^R}{L} \right) \right. \\ &\left. - \frac{c(s) \cos(\tilde{\theta} + \delta_P^R)}{1 - c(s)y} \right] \end{aligned} \quad (9)$$

2) *Control law design*: Since kinematical model (3) with sliding accounted is validated and can be turned into chained form (7), a natural expression for the virtual control law is:

$$m_3 = -K_d a_3 - K_p a_2 \quad (K_p, K_d) \in \mathbb{R}^{+2} \quad (10)$$

since it insures that a_2 obeys the following equation:

$$a_2'' + K_d a_2' + K_p a_2 = 0 \quad (11)$$

Equation (11) establishes the following convergences :

- $a_2 \rightarrow 0$: this is equivalent to $y \rightarrow 0$ (according to the state transformation) and ensures convergence of the vehicle to the path to be followed (null lateral deviation).
- $a_3 \rightarrow 0$: this implies (according to the state transformation) that $\tilde{\theta} \rightarrow \delta_P^R$. This condition shows that the vehicle heading will not be parallel to the reference path tangent, but will compensate effect of rear cornering angle to ensure the convergence of lateral deviation to zero. Vehicle then evolutes crabway.

The actual control variable is vehicle steering angle. It can be obtained by reporting (10) in (9), and inverting the resulting relation. We obtain :

$$\delta = \arctan \left\{ \frac{L}{\cos \delta_P^R} \left[c(s) \frac{\cos \tilde{\theta}_2}{\alpha} + A \frac{\cos^3 \tilde{\theta}_2}{\alpha^2} \right] + \tan \delta_P^R \right\} - \delta_P^R \quad (12)$$

$$\text{where: } \begin{cases} \tilde{\theta}_2 &= \tilde{\theta} + \delta_P^R \\ \alpha &= 1 - c(s)y \\ A &= -K_d \alpha \tan \tilde{\theta}_2 - K_p y + c(s) \alpha \tan^2 \tilde{\theta}_2 \end{cases}$$

Performances of such a control law can be adjusted by tuning gains K_p and K_d which can be viewed as proportional and derivative actions of a linear controller. In experimental results hereafter detailed, gains are set to values (13). They impose a convergence to the reference path within 15m, without overshoot.

$$\begin{cases} K_p &= 0.09 \\ K_d &= 0.6 \end{cases} \quad (13)$$

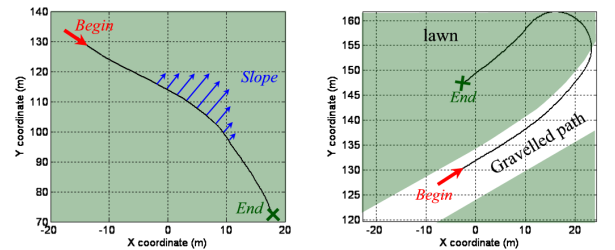
VI. EXPERIMENTAL RESULTS

A. Reference path

The experimental results of the two control laws can be described by the two experiments detailed below. They consist in straight line following on a sloping field at $4km.H^{-1}$ (figure 10(a)) and in curve following on an even sloppy ground at $7km.H^{-1}$ (figure 10(b)). Ground on which vehicle has run is gravel or lawn as depicted on figure 10. These two paths are representative of guidance conditions in which sliding appears and reduces trajectory tracking accuracy. Performances are compared with control law without sliding accounted (4).

B. Results on lateral deviation

Figure 11 depicts the straight line following on sloping ground. Classical control without sliding accounted makes vehicle converge up to a non null deviation during slope (ie



(a) Straight line on slope

(b) Half circle

Fig. 10. Actual paths to be followed

when sliding occurs). On the contrary, with both of control laws with sliding accounted, lateral deviation comes back to zero during slope. Their performances are very similar: as slope appears, one can observe a transient deviation before sliding models can supply relevant information.

Such a delay to calculate relevant values for sliding parameters when these latter change quickly appears more significantly on figure 12 which depicts curved path following. At the beginning and the ending of the curve, curvature introduces a step on sliding parameters, and the brief non negligible lateral deviation observed is due to control laws settling time. This effect is amplified as in both of control law, sliding is considered as constant or slow varying, what appears to be not relevant as vehicle beginning or ending a curve ($\dot{\theta}$ and δ are not constants). Sliding effects are then significantly compensated during the curve, but overshoots at transient phases have now to be addressed. Overshoot are so amplified than there is a hardware delay on low level steering actuator

It can however be noticed that new control law using TBD Model (12) is able to react faster since sliding parameters are included inside nonlinear control calculation. In this critical path following where curvature radius is close to tractor maximal one (steering angle control δ goes up to 40°), the less reactive method (adaptive control using VBD Model) is not able to steer the tractor to a null lateral deviation during such a curve.

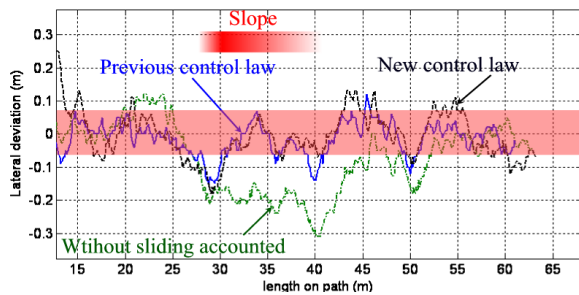


Fig. 11. Lateral deviation during sloping path following

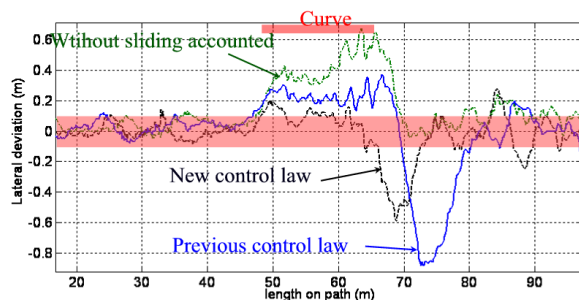


Fig. 12. Lateral deviation during curved path following

VII. CONCLUSION AND FUTURE WORKS

In this paper two vehicle kinematic models accounting for sliding effects are described. It has been shown that they can fit with actual vehicle dynamics and are equivalent to

describe vehicle behavior. However structure of these models are different and control scheme designed using one or other model is then different. As expected, control scheme developed using TBD model is theoretically and actually faster, as sliding parameters are entered inside control calculation.

One limitation of such laws is the impact of noise resulting from vehicle dynamical movement (cabin oscillation, since GPS antenna is located on the top of the tractor). Butterworth filters are presently used to smooth sliding parameters estimation, but they are not fully satisfactory. Another critical point appears when sliding parameters are quickly modified (typically at the beginning/ending of a curve). Since sliding parameters are assumed to be constant, and considering time delay due to sliding estimation and low level actuator capacities, a transient deviation then occurs.

Current developments are focused on these problems. Predictive control methods are investigated to take into account time varying sliding and low level delay to eliminate overshoot problems especially in curve. Adaptive filters are in development to reject parasite dynamical movements which depend on ground conditions and configuration of tractor (implement loaded on tractor...). Such additional principles will have to improve guidance control in presence of sliding in all tractor configurations and for any paths to be followed, ground conditions, to meet farmer expectations (about $\pm 5cm$).

REFERENCES

- [1] Ackermann J.. *Robust Lateral and Yaw Control*. In Proc. of Eur. summer school in automatic control, Grenoble (France), 2002.
- [2] Dormegnien E., Fandard G., Mahajoub G., Zarka F.. *Dynamique du véhicule*. Lectures at French Institute for Advanced Mechanics (IFMA), 2002.
- [3] Ellouze M. and d'Andréa-Novel B.. *Control of unicycle-type robots in the presence of sliding effects with only absolute longitudinal and yaw velocities measurement*. In European Journal of Control, 6:567-584, 2000.
- [4] Holzhüter T. and Schultze R.. *Operating experience with a high-precision track controller for commercial ships*. In Control Engineering Practice 4(3):343-350, 1996.
- [5] Lenain R., Thuilot B., Cariou C. and Martinet P.. *Adaptive control for car like vehicles guidance relying on RTK GPS: rejection of sliding effects in agricultural applications*. In Proc. of the Intern. Conf. on Robotics and Automation (ICRA), Taipei, Sept. 2003.
- [6] Micaelli A., Samson C.. *Trajectory tracking for unicycle-type and two-steering-wheels mobile robots*. INRIA research report Number 2097, Nov. 1993.
- [7] Nagasaka Y., Otani R., Shigeta K. and Taniwaki K.. *Automated operation in paddy fields with a fiber optic gyro sensor and GPS*. In Proc. of the Intern. Workshop on Robotics and Automated Machinery for Bio-Productions (Bio-Robotics), pp 21-26, Valencia (Spain) September 1997.
- [8] O'Connor M., Elkaim G., Bell T. and Parkinson B.. *Automatic steering of a farm vehicle using GPS*. In Proc. of the 3rd Intern. Conf. on Precision Agriculture, Minneapolis (USA), pp 767-777, June 1996.
- [9] Ried J. and Niebuhr D.. *Driverless tractors*. In Ressource 8(9):7-8, September 2001.
- [10] Samson C.. *Control of chained systems. Application to path following and time-varying point-stabilization of mobile robots*. In IEEE Trans. on Automatic Control 40(1):64-77, January 1995.
- [11] Stentz A, Dima C, Wellington C, Herman H, Stager D *A system for semi-autonomous tractor operations* in Autonomous robots 13(1):87-104, 2002.
- [12] Thuilot B., Cariou C., Martinet P. and Berducat M.. *Automatic guidance of a farm tractor relying on a single CP-DGPS*. In Autonomous robots 13(1):53-71, July 2002.
- [13] The Zodiac. *Theory of robot control*. Canudas de Wit C., Siciliano B. and Bastin G. eds, Springer Verlag, Berlin (Germany) 1996.